Off-plane polarization ordering in metal chalcogen diphosphates from bulk to monolayer

Wenshen Song,[1] Ruixiang Fei,[1] and Li Yang[1,2,*]

[1]*Department of Physics, Washington University in St. Louis, St. Louis, Missouri 63130, USA*
[2]*Institute of Materials Science and Engineering, Washington University in St. Louis, St. Louis, Missouri 63130, USA*

Vertically (off-plane) ferroelectric ordering in ultrathin films has been pursued for decades. We predict the existence of intrinsic vertical polarization orderings in ultrathin metal chalcogen-diphosphates (MCDs). Taking $CuInP_2Se_6$ as an example, the first-principles calculation and electrostatic-energy model show that, under the open-circuit boundary condition, the ground state of bulk $CuInP_2Se_6$ is ferroelectric (FE) while that of monolayer is antiferroelectric (AFE), and the critical thickness for this FE/AFE transition is around six layers. Interestingly, under the closed-circuit boundary condition, the FE state can hold even for monolayer. Particularly, because of the small energy difference but the large barrier between FE and AFE orderings, the FE state can be stabilized in a free-standing monolayer, giving rise to intrinsic, off-plane two-dimensional ferroelectrics. Applying Monte Carlo simulations, we further calculate the ferroelectric Curie temperature (T_c) and electric hysteresis.

I. INTRODUCTION

Ferroelectrics, arising from macroscopic polarization induced by spontaneous ordering of electric dipoles and switchable under external electric field, has attracted extensive attention. The ultrathin ferroelectric (FE) films are obviously the most useful structure for exploring new physics and realizing device applications, such as FE transistors and memories [1]. To date most works on ferroelectrics have focused on perovskite oxides, such as $PbTiO_3$ and $BaTiO_3$ [2–9]. Unfortunately, their ferroelectricity is extremely sensitive to vertical boundary conditions [10,11]. As a result, drastic depolarization effects emerge in these three-dimensional structures when they are thinned down, resulting in a suppression of polarization and thus a critical thickness for sustaining the FE state [12,13]. Realizing ultrathin ferroelectricity is thus known hard to achieve.

Layered van der Waals (vdW) materials may give hope to overcoming this challenge. Two-dimensional (2D) in-plane ferroelectricity has been predicted and observed in monolayer group IV monochalcogenides [14–17]. This ignites novel applications, such as giant piezoelectricity [18,19], bulk photovoltaics, and photostriction [20,21]. However, the more useful off-plane (vertical) ferroelectricity is still challenging. More recently, a few layered materials have been theoretically predicted to be vertically ferroelectric, such as In_2Se_3 [22], 1T-phase MoS_2 [23], and Sc_2CO_2 with 2D electron/hole [24], although many of these structures are metastable or the ferroelectricity is not intrinsic. On the other hand, experiments reported that metal chalcogen-diphosphates (MCDs) can be a promising family of ultrathin FE materials: Ferroelectricity is observed in a fabricated bilayer [25]. This may shed light on intrinsically stable 2D structures with off-plane ferroelectricity. However, other measurements claim that ferroelectricity can only exist in samples with much larger thickness of MCDs [26,27].

In this work, we take $CuInP_2Se_6$ [Fig. 1(a)], a typical member of the family of layered vdW MCDs, as an example

and show that monolayer MCD may sustain a polarization ordering even down to the monolayer. Unlike bulk $CuInP_2Se_6$ which is always FE, we reveal that the vertical boundary conditions are crucial for determining the polarization orders of ultrathin structures: The freestanding (open-circuit) monolayer $CuInP_2Se_6$ is antiferroelectric (AFE) but the closed-circuit (shortcut) monolayer can hold the FE phase as the ground state. Particularly, given the substantial transition energy barrier between AFE and FE states, the FE state can be held as a robustly metastable state of the free-standing monolayer, giving rise to 2D vertical ferroelectricity. Finally, the FE phase transition temperature and electric hysteresis curves of the free-standing monolayer $CuInP_2Se_6$ are obtained by Monte Carlo (MC) simulations [28].

The remainder of this paper is organized as follows: In Sec. II, we introduce the calculation methods and parameters of simulations. In Sec. III, we present the polarization orders in monolayer and bulk $CuInP_2Se_6$, respectively. Particularly, the question of boundary conditions and polarization is raised. In Sec. IV, to mimic different boundary conditions, an electrostatic-energy model is built and a detailed discussion of how to fit the relevant parameters is presented. In Sec. V, with the model and first-principles calculation, the critical thickness for the FE/AFE transition is predicted. In Sec. VI, we discuss the polarization orders and transition barriers between the FE and AFE states under the free-standing boundary condition. In Sec. VII, the FE Curie temperature and the hysteresis are presented after considering finite temperature. In Sec. VIII, we summarize our studies and conclusion.

II. COMPUTATIONAL METHODS

The relaxed atomistic structures and electronic structures are calculated by density functional theory (DFT) with the generalized gradient approximation using the Perdew-Burke-Ernzerhof (GGA-PBE) functional [29], implemented in the Vienna *ab initio* simulation package (VASP) [30,31]. The VdW interaction is included through the DFT-D2 method of Grimme [32]. The energy cutoff is 600 eV for structure relaxation and solving the Kohn-Sham equation. We use a $6 \times 6 \times 1$ k-grid sampling in the reciprocal space. A vacuum distance is set to

*lyang@physics.wustl.edu
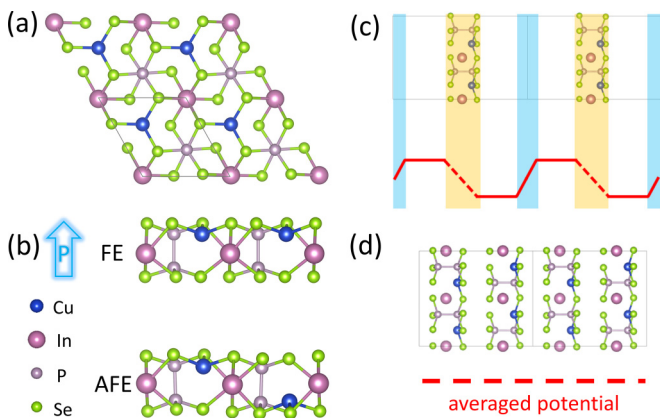
FIG. 1. (a) Top view of monolayer $CuInP_2Se_6$. (b) Side views of the FE (upper) and AFE (lower) states. (c) Schematic potential of FE monolayer under the $D = 0$ (open-circuit) boundary condition. (d) Averaged electric potential of bulk under the $E = 0$ (closed-circuit) boundary condition.

be larger than 20 Å between adjacent mono/few layer(s) for avoiding spurious interactions. The climbing image nudged elastic band (cNEB) method [33,34] is employed to calculate the transition states and minimum energy path (MEP). The polarization is obtained by the modern theory of polarization based on the Berry-phase approach [35,36]. As a validation, we have used the Berry-phase method to calculate spontaneous polarization of a typical MCD FE material, bulk $CuInP_2S_6$ (CIPS), which is 3.20 $\mu C/cm^2$. This is in good agreement with experimental measurements [37], which is 3.5 $\mu C/cm^2$ at 153 K, 3.0 $\mu C/cm^2$ at room temperature, and 2.55 $\mu C/cm^2$ from hysteresis at room temperature.

For the Monte Carlo (MC) simulation [28], the length of steps is set to be 0.2 Å and the number of steps is 20 000. We randomly pick up the direction (positive/negative) of each step with even probability and determine the acceptance using the Metropolis-Hastings algorithm [28]. This process is repeated for about 50 times with a fixed starting point and use the average of final positions as a result. Finally, the whole process is repeated for about 100 times to obtain the converged mean values and standard deviations for estimating error bars. We have verified these simulation parameters by comparing the MC-calculated Curie temperature with the measured values of bulk $CuInP_2Se_6$.

III. POLARIZATIONS AND BOUNDARY CONDITIONS

As shown in Fig. 1(b), $CuInP_2Se_6$ has two typical low-energy structures: One is the FE ordering with all copper atoms at the same side, which is its known bulk structure that exhibits a ferroelectric ground state [37,38]; the other is the AFE ordering with copper atoms arranged in a line-by-line, up-and-down pattern. This is also a popular structure of many other MCDs, such as bulk $CuCrP_2Se_6$ [38]. Our first-principles calculation confirms that the FE state of bulk $CuInP_2Se_6$ is more stable than the AFE state by an energy difference of ~13 meV/formula unit (f.u.). For the freestanding monolayer $CuInP_2Se_6$, we find that, however, the energy of the AFE state is about 12 meV/f.u. less than FE, making AFE be

the rigorously ground state of the monolayer due to the depolarization effect. In other words, at very low temperature and under perfect equilibrium, the freestanding monolayer $CuInP_2Se_6$ will theoretically stay on an AFE order or form dipole glass [39–41].

Since the ground state of bulk $CuInP_2Se_6$ is FE while that of the monolayer is AFE, an obvious question is to find the critical thickness for this FE/AFE transition. Answering this question leads us to a subtle while crucial problem: The above first-principles calculations of bulk and slab structures are actually performed under different boundary conditions, which are, unfortunately, an essential factor to decide the polarization ordering and depolarization effect. In slab structures, as shown in Fig. 1(c), the existence of a vacuum between layers makes it possible to keep the periodic boundary condition by applying a dipole correction only in the vacuum region [42]. This mimics the freestanding case (the open-circuit boundary condition). However, to keep the periodic boundary condition of bulk structures [Fig. 1(d)], the overall electric field of bulk must be zero ($E = 0$) and *ab initio* packages always automatically apply a compensating field to cancel the spontaneous polarization field. In other words, this mimics the closed-circuit boundary condition [11]. In this sense, our above calculated total energies of bulk and monolayer are under different boundary conditions and the claim for their ground states is problematic. Especially, a brute-force first-principles calculation cannot mimic the open-circuit ($D = 0$) boundary condition for bulk FE structures because of they are periodic without vacuum.

IV. ELECTROSTATIC-ENERGY MODEL

To solve this problem and compare the total energy within the same boundary condition, we introduce an electrostatic-energy model to investigate ground states and ferroelectricity under electric field [10]. This model will also pave the way for following MC simulations and studies of hysteresis. Based on the geometry and energy track from the *ab initio* climbing image nudged elastic band (cNEB) method [33,34], we define the displacement of copper atoms from the central position as a polar internal degree of freedom u, which is the displacement of copper atoms. The free energy per f.u. can be expressed as

$$
\begin{aligned}
F(u,E) &= au^2 + bu^4 + cu^6 + E_{es} \\
&= au^2 + bu^4 + cu^6 - \big(P_s(u)E \\
&\quad + \tfrac{1}{2}(\epsilon(u) - 1)\epsilon_0 E^2\big)\Omega.
\end{aligned}
\tag{1}
$$

The first three terms in Eq. (1) form a double-well potential that represents the lattice self-energy described by the Landau theory up to the sixth order. It is called the landau energy part. The rest part (E_{es}) of the free energy represents the electrostatic energy under E field, which is defined as E_{es}. Ω is the volume of an f.u. and ϵ is the electric permittivity.

In solids, the total polarization can be written as

$$
P = -\frac{\partial F(u,E)}{\Omega \partial E} = P_s(u) + (\epsilon(u) - 1)\epsilon_0 E,
\tag{2}
$$

where $P_s(u)$ is spontaneous polarization under $E = 0$, merely depending on the displacement u of copper atoms in our studied $CuInP_2Se_6$ structure. The second term is the electronic

TABLE I. Fitted parameters of the Landau energy in Eq. (1).

Layer	a (meV/A^2)	b (meV/A^4)	c (meV/A^6)
1	-131.10	16.97	26.16
Bulk	-168.13	33.31	16.92

correspondence to the electric field E, in which $\epsilon(u)$ is the ion-clamped relative permittivity, which can be calculated by first-principles simulations. Therefore, combining with the general relationship, $D = \epsilon_0 E + P$, we can realize different electric boundary conditions by this electrostatic-energy model.

The parameters in Eq. (1) can be obtained for bulk and slab structures, respectively. For the bulk structure, the relative permittivity can be directly calculated by DFT based on the random-phase approximation (RPA) [43,44]. Moreover, because of the periodic boundary condition, the overall electric field E must be zero. As a result, the electrostatic energy part of Eq. (1) disappears and we only need to handle the Landau energy. These parameters can be obtained by fitting the first-principles calculated free energy according to the displacement of copper atoms. The fitted parameters of bulk CuInP$_2$Se$_6$ are concluded in Table I.

For slab structures including monolayer and few layers, the fitting process is slightly more complicated. First, we must find the relative permittivity. Using the relation between electric displacement and polarization,

$$P = \frac{[\epsilon(u) - 1]D + P_s}{\epsilon(u)}, \qquad (3)$$

we can tune the applied electric displacement field in first-principles simulations to get the polarization and corresponding electric permittivity. Given that dielectric function is a linear-response property, we confine our calculation within a weak-field limit, such as around 0.1 V/nm. Within this range of applied field, the first-principles calculation shows that the position of copper atoms is nearly fixed. This substantially simplifies the calculation.

Therefore, we can fix the copper atom displacement u and tune the applied field D. With the calculated polarization P from first-principles Berry-phase calculations, the relative permittivity can be fitted by using Eq. (3). For example, that of monolayer CuInP$_2$Se$_6$ is about 2.58 for the FE phase. Interestingly, we observe a substantial change of the relative permittivity according to the thickness of FE structures, which can be seen from the concluded Table II. Finally, with these fitted $\epsilon(u)$ and the DFT-calculated free energy, we can fit the parameters of the Landau-energy part. Those fitted parameters of the Landau energy of the monolayer are summarized in Table I as well.

TABLE II. Energy difference $E_{FE} - E_{AFE}$ (meV/f.u.) for monolayer and bulk CuInP$_2$Se$_6$ under $D = 0$ and $E = 0$.

Layer	$D = 0$	$E = 0$
1	12.1	-0.03
Bulk	-0.8	-13.2
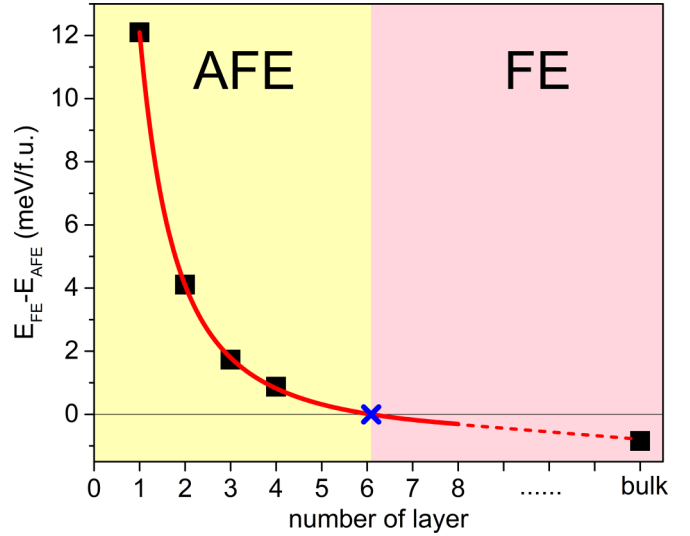
FIG. 2. Layer-dependent evolution of the energy difference ($E_{FE} - E_{AFE}$) of CuInP$_2$Se$_6$ under the $D = 0$ boundary condition. The critical thickness is marked by the cross sign.

V. THE CRITICAL THICKNESS OF THE AFE/FE TRANSITION

With fitted parameters in Eq. (1), we ultimately obtain the FE energy of bulk CuInP$_2$Se$_6$ under the open-circuit boundary condition ($D = 0$). Interestingly, the FE state is still the ground state but its energy is only about 0.8 meV below the AFE state, as shown in Table II. More interestingly, under the other boundary condition, i.e., the closed-circuit case ($E = 0$), the above electrostatic model predicts that the energy of the FE state is always lower than that of the AFE state, indicating that monolayer CuInP$_2$Se$_6$ can be FE when it is shortcut. This is because, under the closed-circuit boundary condition, a compensating electric field always tends to further lower the energy of the FE state, while the AFE configuration holds $D = E = 0$ intrinsically. In this sense, it is necessary to specify the boundary condition when deciding the ground state of vertically polarized 2D structures.

Combining the energy calculated by the electrostatic model of bulk with the first-principles results of mono-/few-layer CuInP$_2$Se$_6$, we finally obtain the layer-dependent evolution of stability of CuInP$_2$Se$_6$ under the open-circuit (freestanding) boundary condition in Fig. 2. Here, we fit the energy relationship with the thickness and find that there is a AFE/FE transition of the ground state for the freestanding six-layer ($\sim$4 nm) CuInP$_2$Se$_6$. Therefore, for free-standing CuInP$_2$Se$_6$, under perfect equilibrium, ultrathin structures shall be AFE.

Finally, with this electrostatic model, we can also calculate the evolution of polarization intensity of CuInP$_2$Se$_6$ according to the thickness, under different electric boundary conditions, as listed in Table III. Importantly, we can see that the boundary condition plays a significant role in deciding the magnitude of spontaneous polarization. As previously mentioned, open circuit ($D = 0$) represents a lack of external field for slab structures. Thus, deviation of centers of ions and electronic charge tend to move with same amplitude as P/ϵ_0 but along opposite directions. This leads to a negative feedback

TABLE III. Layer-dependent thickness, polarization, and relative permittivity (first principle/model) under different boundary conditions.

| Layer | Thickness (Å/f.u.) | Polarization ($\mu C/cm^2$) | | ϵ |
		$D = 0$	$E = 0$	
1	9.00	0.322	0.847	2.62
2	7.82	0.324	1.222	3.77
3	7.80	0.322	1.429	4.44
4	7.23	0.320	1.515	4.73
Bulk	6.64	0.365	2.531	6.93

corresponding to a smaller polarization, i.e., the depolarization effect. Interestingly, for our studied vdW layered $CuInP_2Se_6$, its depolarization effect is not sensitive to the thickness, which is evidenced by the nearly fixed polarization shown in Table III. This is in rather contrast to the widely accepted wisdom learned from non-vdW FE materials, in which the depolarization effect is enhanced in thin films. On the other hand, under the closed-circuit ($E = 0$) boundary condition, the depolarized field is compensated by the external field, endowing centers of ions and electronic charge with much more freedom to move away from each other. Therefore, larger polarization is generally observed.

VI. POLARIZATION IN FREESTANDING $CuInP_2Se_6$

In the following, we particularly focus on polarization orderings in monolayer $CuInP_2Se_6$ under the open-circuit boundary condition, which is the intrinsic case of freestanding samples. Importantly, despite the AFE ground state, the FE state can be a robustly metastable state in realistic monolayer $CuInP_2Se_6$. As shown in Fig. 3(a), our first-principles NEB simulation shows that the energy barriers from the FE states to the AFE state are significant, e.g., ~80 meV for monolayer and ~120 meV for bulk. On the other hand, the energy difference between the AFE and FE state is much smaller (~10 meV). In other words, both FE and AFE states could coexist due to this large energy barrier. It agrees with the experimental fact that, despite the FE ordering is the ground state, bulk $CuInP_2Se_6$ exhibits dipole-glass properties at low temperature, because of a mixture of FE and AFE orderings [39–41]. In other words, if a strong initialing field is applied to forcing an FE ordering, the vertically ferroelectricity may be stable and observed in monolayer $CuInP_2Se_6$ because of the significant energy barrier between the FE and AFE states. This gives hope to practically monolayer FE structures.

Our results may be useful for understanding recent measurements of few-layer MCDs. For example, recent experiments have reached controversial conclusions of the existence of the FE state in few-layer $CuInP_2S_6$ (CIPS) [25–27], a material very similar to our studied $CuInP_2Se_6$: Ferroelectricity was reported in bilayer CIPS [25] but other measurements showed an opposite conclusion [26,27]. We have calculated spontaneous polarization of mono-/few-layer CIPS. Nearly the same energetic pictures have been obtained. Therefore, on one hand, with a strong initial field, the FE state can be formed and observed due to the larger energy barrier between the AFE and FE states. On the other hand, if without a strong enough initial
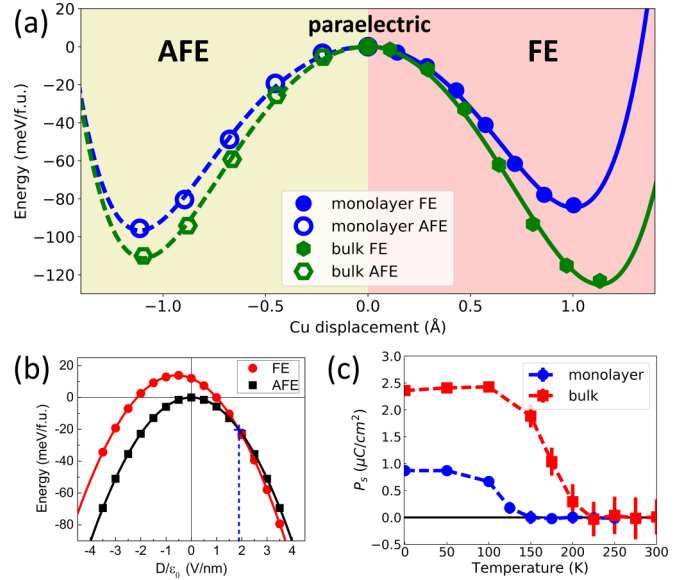
FIG. 3. (a) Monolayer and bulk sample FE(AFE)-to-paraelectric energy tracks from first-principles NEB calculations. (b) Energy variation with aspect to the applied displacement field D/ϵ_0. The energy of the FE state of the freestanding monolayer is set to be zero. (c) Temperature-dependent zero-E-field spontaneous polarization P_s in monolayer and bulk $CuInP_2Se_6$.

field, a likely coexistence of AFE and FE domains may lead to a dipole glass state and, thus, eliminate the macroscopic polarization.

Furthermore, first-principles simulations can provide the energetic stability of different orderings under the applied external field, as shown in Fig. 3(b). The energy vs electric field is perfectly fitted by a quadratic function, confirming our electrostatic-energy model in Eq. (1). As expected, when an external field is applied to the slab along the direction of spontaneous polarization, FE energy will decrease with a higher rate than AFE. If comparing with the same external field, when D/ϵ_0 exceeds 1.9 V/nm marked by a blue cross in Fig. 3(b), FE energy will be lower than that of AFE. This corresponds to a critical situation that the ground state transforms from the AFE state to the FE state at 0 K under full equilibrium.

VII. POLARIZATION UNDER FINITE TEMPERATURE

In addition to spontaneous polarization, ferroelectricity requires the polarization can be switched by practical external field. In this sense, the coercive field is crucial for deciding the feasibility of our predicted ferroelectricity. At very low temperature, because of the large energy barrier shown in Fig. 3(a), the coercive field to switch these spontaneous polarizations in $CuInP_2Se_6$ could be very large. For example, for bulk one, our calculation shows that its coercive field is about 14 V/nm, which is too large compared with experimental value of 77 kV/cm [37]. On the other hand, previous first-principles calculations revealed the similar size of energy barriers in many other known ferroelectric materials [10,45], whose practically coercive fields are, however, much smaller in reality.
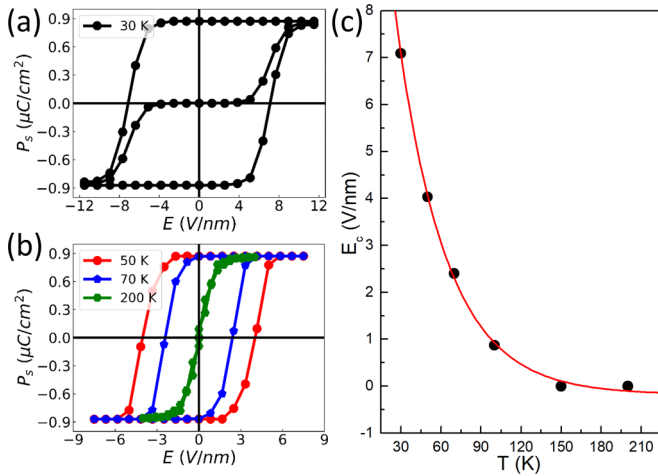
FIG. 4. (a) Electric hysteresis of polarization of monolayer $CuInP_2Se_6$ under 30 K, starting from the AFE ground state, then evolving into and stabilizing at the FE state. (b) Electric hysteresis of FE $CuInP_2Se_6$ P_s under different temperatures. (c) Temperature-dependent coercive field with an exponential decay fitting.

There are several reasons, such as ferroelectric domains [46,47], that can contribute to this lower coercive field for sizable energy barriers. Here we focus on the temperature effect. In a realistic condition, finite temperature can substantially reduce the coercive field. To include the temperature effect and further show the important hysteresis, the MC method is thus applied. Particularly, because of small interactions between two adjacent units in both FE and AFE states, which can be seen from the small energy difference between AFE/FE states [Fig. 3(a)], our MC simulation within a single or double unit cell can reflect the properties of the FE and FE orderings, respectively. The MC simulated results are presented in Fig. 3(c). Based on the effective Hamiltonian [Eq. (1)] with fitted parameters of bulk $CuInP_2Se_6$, MC gives a transition temperature around 225 K, which agrees well with experimental values $220 \sim 240$ K of bulk $CuInP_2Se_6$ [48,49]. Using the fitted parameter of monolayer $CuInP_2Se_6$, we estimate the Curie temperature to be around 150 K for the monolayer. This smaller T_c is mainly from the smaller energy barrier of the monolayer, as shown in Fig. 3(a).

Finally, using this MC approach, we can simulate the electric hysteresis of monolayer $CuInP_2Se_6$. Because the initial AFE state has opposite polarizations between neighbored units, an average of two unit cells of the MC process with a different starting position can simulate the AFE to FE transition under finite temperature. Figure 4(a) shows that, with the added electric field [applying our electrostatic-energy model in Eq. (1)] at 30 K, the AFE ground state will gradually evolve into a commensurate state, since electric field will

mandatorily tilt the double-well potential. In fact, this field that forces the AFE-to-FE phase transition has been observed in bulk $Pb(Zr,Sn,Ti)O_3$ experimentally [50] and provides a useful way to obtain the FE state from the AFE ground state. In Fig. 4(b), we present how the hysteresis evolves with the temperature. At 30 K, the coercive field is 7.1 V/nm; at 100 K the value decreases to 0.9 V/nm; finally, at 200 K, hysteresis degrades into a single-value curve because the ferro-to-para phase has occurred at the Curie temperature of 150 K. In other words, as temperature increases, the coercive field will reduce rapidly until it reaches the transition temperatures [50,51]. We have concluded the relation between the coercive field and the temperature in Fig. 4(c), which is roughly fitted by an exponential curve. We can see that, if the temperature is above 100 K, this spontaneous FE ordering can be switchable under the practical field (less than 1 V/nm), making it promising to realize and use ferroelectricity in monolayer $CuInP_2Se_6$.

VIII. SUMMARY

In conclusion, we have clarified two important boundary conditions that are essential for deciding energy and polarization orderings in bulk and slab structures. With first-principles simulations and the electrostatic-energy model, we predict robust off-plane polarization orderings in ultrathin films of a promising family of materials, MCDs. Taking $CuInP_2Se_6$ as an example, under the (freestanding) open-circuit boundary condition, the ground state of bulk is FE while that of the monolayer is switched to be AFE, and the critical thickness for the AFE/FE transition is predicted to be six layers; however, under the closed-circuit boundary condition, the ground state of both bulk and monolayer is always FE. Moreover, even for freestanding mono-/few-layer CuInP2Se6, because of the small energy difference and large barrier between AFE and FE states, the FE state can be practically stabilized and useful for devices. Finally, using MC, we explore the Curie temperature and electric hysteresis, indicating that the corresponding coercive field is well within the practical range at finite temperature. Our studies are useful for understanding recent controversial measurements and further shedding light on ferro-/antiferro-electricity in ultrathin vdW materials.

[1] J. F. Scott, *Ferroelectric Memories*, Vol. 3 (Springer Science & Business Media, New York, 2013).

[2] R. D. King-Smith and D. Vanderbilt, Phys. Rev. B **49**, 5828 (1994).

[3] W. J. Merz, J. Appl. Phys. **27**, 938 (1956).

[4] R. E. Cohen, Nature (London) **358**, 136 (1992).

[5] J. B. Neaton, C. Ederer, U. V. Waghmare, N. A. Spaldin, and K. M. Rabe, Phys. Rev. B **71**, 014113 (2005).

[6] S. Liu, I. Grinberg, and A. M. Rappe, Nature (London) **534**, 360 (2016).

[7] N. A. Benedek and C. J. Fennie, J. Phys. Chem. C **117**, 13339 (2013).

[8] L. Chen, Y. Yang, Z. Gui, D. Sando, M. Bibes, X. K. Meng, and L. Bellaiche, Phys. Rev. Lett. **115**, 267602 (2015).

[9] H. Xiang, Phys. Rev. B **90**, 094108 (2014).

[10] K. F. Garrity, K. M. Rabe, and D. Vanderbilt, Phys. Rev. Lett. **112**, 127601 (2014).

[11] M. Stengel, N. A. Spaldin, and D. Vanderbilt, Nat. Phys. **5**, 304 (2009).

[12] J. Junquera and P. Ghosez, Nature (London) **422**, 506 (2003).

[13] M. Stengel, D. Vanderbilt, and N. A. Spaldin, Nat. Mater. **8**, 392 (2009).

[14] R. Fei, W. Kang, and L. Yang, Phys. Rev. Lett. **117**, 097601 (2016).

[15] P. Z. Hanakata, A. Carvalho, D. K. Campbell, and H. S. Park, Phys. Rev. B **94**, 035304 (2016).

[16] M. Wu and X. C. Zeng, Nano Lett. **16**, 3236 (2016).

[17] K. Chang, J. Liu, H. Lin, N. Wang, K. Zhao, A. Zhang, F. Jin, Y. Zhong, X. Hu, W. Duan *et al.*, Science **353**, 274 (2016).

[18] R. Fei, W. Li, J. Li, and L. Yang, Appl. Phys. Lett. **107**, 173104 (2015).

[19] L. C. Gomes, A. Carvalho, and A. H. Castro Neto, Phys. Rev. B **92**, 214103 (2015).

[20] T. Rangel, B. M. Fregoso, B. S. Mendoza, T. Morimoto, J. E. Moore, and J. B. Neaton, Phys. Rev. Lett. **119**, 067402 (2017).

[21] R. Haleoot, C. Paillard, T. P. Kaloni, M. Mehboudi, B. Xu, L. Bellaiche, and S. Barraza-Lopez, Phys. Rev. Lett. **118**, 227401 (2017).

[22] W. Ding, J. Zhu, Z. Wang, Y. Gao, D. Xiao, Y. Gu, Z. Zhang, and W. Zhu, Nat. Commun. **8**, 14956 (2017).

[23] S. N. Shirodkar and U. V. Waghmare, Phys. Rev. Lett. **112**, 157601 (2014).

[24] A. Chandrasekaran, A. Mishra, and A. K. Singh, Nano Lett. **17**, 3290 (2017).

[25] F. Liu, L. You, K. L. Seyler, X. Li, P. Yu, J. Lin, X. Wang, J. Zhou, H. Wang, H. He *et al.*, Nat. Commun. **7**, 12357 (2016).

[26] A. Belianinov, Q. He, A. Dziaugys, P. Maksymovych, E. Eliseev, A. Borisevich, A. Morozovska, J. Banys, Y. Vysochanskii, and S. V. Kalinin, Nano Lett. **15**, 3808 (2015).

[27] M. Chyasnavichyus, M. A. Susner, A. V. Ievlev, E. A. Eliseev, S. V. Kalinin, N. Balke, A. N. Morozovska, M. A. McGuire, and P. Maksymovych, Appl. Phys. Lett. **109**, 172901 (2016).

[28] M. Newman and G. Barkema, *Monte Carlo Methods in Statistical Physics* (Oxford University Press, New York, 1999), Chap. 1–4.

[29] J. P. Perdew, K. Burke, and M. Ernzerhof, Phys. Rev. Lett. **77**, 3865 (1996).

[30] G. Kresse and J. Furthmüller, Phys. Rev. B **54**, 11169 (1996).

[31] G. Kresse and D. Joubert, Phys. Rev. B **59**, 1758 (1999).

[32] S. Grimme, J. Comput. Chem. **27**, 1787 (2006).

[33] H. Jónsson, G. Mills, and K. W. Jacobsen, in *Classical and Quantum Dynamics in Condensed Phase Simulations* (World Scientific, Singapore, 1998), Chap. 16, pp. 385–404.

[34] G. Henkelman, B. P. Uberuaga, and H. Jónsson, J. Chem. Phys. **113**, 9901 (2000).

[35] R. D. King-Smith and D. Vanderbilt, Phys. Rev. B **47**, 1651(R) (1993).

[36] R. Resta, Rev. Mod. Phys. **66**, 899 (1994).

[37] V. Maisonneuve, V. B. Cajipe, A. Simon, R. Von Der Muhll, and J. Ravez, Phys. Rev. B **56**, 10860 (1997).

[38] X. Bourdon, V. Maisonneuve, V. Cajipe, C. Payen, and J. Fischer, J. Alloys Compd. **283**, 122 (1999).

[39] A. Dziaugys, J. Banys, J. Macutkevic, R. Sobiestianskas, and Y. Vysochanskii, Phys. Status Solidi A **207**, 1960 (2010).

[40] J. Banys, R. Grigalaitis, J. Macutkevic, A. Brilingas, V. Samulionis, J. Grigas, and Y. Vysochanskii, Ferroelectrics **318**, 163 (2005).

[41] M. Maior, L. Belej, M. Gurzan, and Y. M. Vysochanskii, Ferroelectrics **349**, 71 (2007).

[42] L. Bengtsson, Phys. Rev. B **59**, 12301 (1999).

[43] S. Baroni and R. Resta, Phys. Rev. B **33**, 7017 (1986).

[44] M. Gajdoš, K. Hummer, G. Kresse, J. Furthmüller, and F. Bechstedt, Phys. Rev. B **73**, 045112 (2006).

[45] S. P. Beckman, X. Wang, K. M. Rabe, and D. Vanderbilt, Phys. Rev. B **79**, 144124 (2009).

[46] S. Kim, V. Gopalan, and A. Gruverman, Appl. Phys. Lett. **80**, 2740 (2002).

[47] K. Kitamura, Y. Furukawa, K. Niwa, V. Gopalan, and T. E. Mitchell, Appl. Phys. Lett. **73**, 3073 (1998).

[48] J. Banys, V. Samulionis, V. Cajipe, and Y. Vysochanskii, Ferroelectrics **257**, 163 (2001).

[49] K. Moriya, N. Kariya, I. Pritz, Y. M. Vysochanskii, A. Inaba, and T. Matsuo, Ferroelectrics **346**, 143 (2007).

[50] P. Yang and D. A. Payne, J. Appl. Phys. **71**, 1361 (1992).

[51] J. Zhai and H. Chen, Appl. Phys. Lett. **82**, 2673 (2003).